Inhibition of c-Src expression and activation in malignant pleural mesothelioma tissues leads to apoptosis, cell cycle arrest, and decreased migration and invasion

Anne S. Tsao,[1] Dandan He,[1] Babita Saigal,[1] Suyu Liu,[2] J. Jack Lee,[2] Srinivasa Bakkannagari,[1] Nelson G. Ordonez,[3] Waun Ki Hong,[1] Ignacio Wistuba,[1,3] and Faye M. Johnson[1,4]

Departments of [1]Thoracic/Head and Neck Medical Oncology, [2]Biostatistics and Applied Mathematics, and [3]Pathology, The University of Texas M. D. Anderson Cancer Center and [4]The University of Texas Graduate School of Biomedical Sciences, Houston, Texas

Abstract

Malignant pleural mesothelioma (MPM) is a deadly disease with few systemic treatment options. One potential therapeutic target, the non–receptor tyrosine kinase c-Src, causes changes in proliferation, motility, invasion, survival, and angiogenesis in cancer cells and may be a valid therapeutic target in MPM. To test this hypothesis, we determined the effects of c-Src inhibition in MPM cell lines and examined c-Src expression and activation in tissue samples. We analyzed four MPM cell lines and found that all expressed total and activated c-Src. Three of the four cell lines were sensitive by *in vitro* cytotoxicity assays to the c-Src inhibitor dasatinib, which led to cell cycle arrest and increased apoptosis. Dasatinib also inhibited migration and invasion independent of the cytotoxic effects, and led to the rapid and durable inhibition of c-Src and its downstream pathways. We used immunohistochemical analysis to determine the levels of c-Src expression and activation in 46 archived MPM tumor specimens. The Src protein was highly expressed in tumor cells, but expression did not correlate with survival. However, expression of activated Src (p-Src Y419) on the tumor cell membrane was higher in patients with advanced-stage disease; the presence of metastasis correlated with higher membrane ($P = 0.03$) and cytoplasmic ($P = 0.04$) expression of p-Src Y419. Lower levels of membrane expression of inactive c-Src (p-Src Y530) correlated with advanced N stage ($P = 0.02$). Activated c-Src may play a role in survival, metastasis, and invasion of MPM, and targeting c-Src may be an important therapeutic strategy. [Mol Cancer Ther 2007; 6(7):1962–72]

Received 1/24/07; revised 4/11/07; accepted 5/25/07.

The costs of publication of this article were defrayed in part by the payment of page charges. This article must therefore be hereby marked *advertisement* in accordance with 18 U.S.C. Section 1734 solely to indicate this fact.

Requests for reprints: Anne S. Tsao, Department of Thoracic/Head and Neck Medical Oncology, M. D. Anderson Cancer Center, 1515 Holcombe Boulevard, Unit 432, Houston, TX 77030. Phone: 713-792-6363; Fax: 713-792-1220. E-mail: astsao@mdanderson.org

doi:10.1158/1535-7163.MCT-07-0052

Introduction

Malignant pleural mesothelioma (MPM) is a deadly disease that arises from normal mesothelial cells that line the pleural cavity. In the United States, MPM is diagnosed in over 3,500 people per year and typically arises in people who have been exposed to asbestos. The overall median survival duration of MPM patients, regardless of stage, is ~9 to 17 months (1, 2). When surgical resection cannot be done, there are no curative options. The best chemotherapy regimens are palliative, with a response rate of 41% for the most effective regimen and prolongation of median survival from 9 to 12 months (3). There is, therefore, a great need to identify new therapeutic targets and develop more effective therapies for patients with MPM.

One potential therapeutic target is the Src family of nonreceptor tyrosine kinases (SFK), which are involved in multiple signaling cascades in cancer cells. c-Src is the most studied of the SFKs and the one most often implicated in cancer progression. SFKs have multiple substrates that lead to diverse biological effects in cancer cells (4, 5). c-Src contributes to the regulation of both focal adhesions (cell-matrix interactions) and adherens junctions (cell-cell interactions), which are essential mediators of cell adhesion, migration, and invasion. The interaction between c-Src and its substrate focal adhesion kinase (FAK) is essential for normal focal adhesion turnover as well as downstream signaling, which can regulate metalloproteinase production required for cancer cell invasion. In epithelial cancers, c-Src facilitates epithelial-to-mesenchymal transition, which may be important to cancer progression (6, 7). Activation of c-Src promotes angiogenesis in several tumor models. c-Src kinase activity is required for vascular endothelial growth factor (VEGF)–mediated angiogenesis (8). The inhibition of SFKs decreases microvessel density and the production of proangiogenic cytokines (9–11). In pancreatic cancer cells, activation of c-Src led to downstream activation of signal transducers and activators of transcription 3 (STAT3), which binds to the VEGF promoter along with hypoxia-inducible factor-1α (12). c-Src activation is also required for epidermal growth factor receptor (EGFR)–induced VEGF production in pancreatic tumor cells (13). Using both molecular and pharmacologic inhibitors of c-Src, researchers found that the development of lymph node and liver metastases was inhibited in orthotopic tumor models (14). c-Src protein overexpression and activation have been associated with

solid tumor carcinogenesis in several tumor types (15). In addition to its effects on FAK, STAT3, VEGF, and hypoxia-inducible factor-1α, c-Src mediates its biological effect through up-regulation of the antiapoptotic genes *Bcl-XL* and *Mcl-1* (5, 16, 17) and downstream signaling cascades that include growth factor receptor binding protein 2/phosphatidylinositol 3-kinase/protein kinase B (AKT), and p42/p44 mitogen-activated protein kinase (5).

c-Src is regulated by several mechanisms. Intramolecular interactions are dictated by the phosphorylation of Y530. In its inactive state, the c-Src protein is phosphorylated at the Y530 residue. Dephosphorylation of Y530 and phosphorylation of a tyrosine residue in the kinase domain (Y419 in humans) leads to the unfolding of the tertiary structure of c-Src and exposure of the kinase catalytic site (5, 18). Dual phosphorylation at both sites still leads to an active conformation. Studies have identified activating mutations in c-Src exon 12 (codon 531) in rare cases of colon and endometrial cancer that result in loss of the negative regulatory role of Y530 (19–21). Another mechanism of c-Src regulation is activation by cell surface receptors, including growth factor receptors and G protein-coupled receptors. Ligand-mediated activation of various growth factor receptors leads to interaction with c-Src, phosphorylation of Y419, and c-Src kinase activation. These growth factor receptors include EGFR, platelet-derived growth factor receptor, c-Met, ErbB2, fibroblast growth factor receptor, and colony-stimulating factor 1 receptor (18).

Cell motility, invasion, survival, and angiogenesis are important for the progression of MPM. Mesothelioma cells secrete and express VEGF and its receptor (22–31). This suggests a role for SFKs, but few data exist that directly address this issue. I.p. inoculation of chickens with a constitutively active form of c-Src (v-Src) led to diffuse peritoneal mesothelioma (32). Exposure of human T cells to asbestos led to decreased apoptosis and to SFK-dependent up-regulation of the prosurvival molecule STAT3 (33). Disruption of c-Src and FAK interaction via expression of the tumor suppressor *merlin* decreased MPM cell invasion (34). We hypothesized that activation of SFKs contributes to MPM progression and that inhibition of SFKs would lead to decreased MPM cell migration and invasion and be an effective therapeutic strategy for MPM. To study the inhibition of SFKs in MPM, we used a competitive ATP inhibitor of SFKs, dasatinib. Dasatinib is a thiazole-based dual Src/Abl kinase inhibitor. The IC_{50} values for Bcr-Abl and SFKs were ≤1.1 nmol/L in an *in vitro* (cell-free) kinase assay (Fyn, 0.2 nmol/L; Src, 0.5 nmol/L; Lck, 1.1 nmol/L; Yes, 0.4 nmol/L; ref. 35). At higher concentrations, dasatinib inhibits various other kinases. Dasatinib is well tolerated in humans and is approved for the treatment of leukemia (36). We tested the effects of dasatinib on four human MPM cell lines and examined the expression and activation of c-Src in 46 human tumor specimens. This is the first publication to investigate the role of SFK inhibition in MPM.

Materials and Methods

Materials

Dasatinib was provided by Bristol-Myers Squibb and was prepared as a 10 mmol/L stock solution in DMSO. [Preliminary cell culture studies have shown that DMSO (≤0.2% was the maximum amount used to deliver dasatinib) has no effect on cell viability, cell cycle, apoptosis, or signaling (data not shown).] The following antibodies were used in Western blot analysis: mitogen-activated protein kinase and phosphorylated mitogen-activated protein kinase (Promega); phosphorylated AKT (New England Biolabs); c-Src (Santa Cruz Biotechnology); pY419-c-Src, p27, pY705-STAT3, STAT3, and cyclin D1 (Cell Signaling Technology); pY861-focal adhesion kinase (FAK; BioSource); FAK (Upstate Biotechnology); and actin (Sigma Chemical Company). Matrigel and Annexin V were purchased from BD Biosciences. Antibodies for immunohistochemistry consisted of anti-rabbit polyclonal antibodies specific for c-Src-p-SRC family Y416 and Y527 (Cell Signaling Technology). The polyclonal Y416 antibody cross-reacts with human tissue at Y419, and the Y527 antibody cross-reacts with human tissue at Y530.

Cell Culture

Four human MPM cell lines (MSTO-211H, NCI-H28, NCI-H2052, and NCI-H2452) were used in the cell culture studies; all were obtained from American Type Culture Collection. Cells were grown in monolayer cultures in RPMI 1640 containing 10% fetal bovine serum, 2 mmol/L glutamine, and 1 mmol/L sodium pyruvate at 37°C in a humidified atmosphere of 95% air and 5% CO_2. Conditioned medium was obtained from 3T3 cells grown in serum-free DMEM.

Crystal Violet Staining

To assess the effect of dasatinib on cell numbers, we plated cells into 96-well plates and incubated them for 24 h under the conditions described above for standard cell culture maintenance. The cells were subsequently exposed to dasatinib at various concentrations for 72 h. Eight wells were treated at each concentration. Medium was removed from the 96-well plates, and adherent cells were fixed and stained with crystal violet (0.5% crystal violet and 20% methanol) for 30 min. The plates were washed with distilled water, and the stains were extracted with Sorenson's buffer [0.1 mol/L sodium citrate (pH 4.2) and 50% ethanol] overnight at 4°C (37). The absorbance of individual wells was read at 570 nm. The results are reported as the ratio of the average absorbance value in treated cells to the average absorbance value in eight replicate controls. Median effect values (D_m or IC_{50} values) were calculated using Calcusyn Software (Biosoft) and the following median effect equation: $D = D_m [f_a / 1 - f_a]^{1/m}$.

3-(4,5-Dimethylthiazol-2-yl)-2,5-Diphenyltetrazolium Bromide Assay

To confirm the results of the crystal violet assays, we did 3-(4,5-dimethylthiazol-2-yl)-2,5-diphenyltetrazolium (MTT) assays because they include floating and poorly adherent cells that are lost in the crystal violet assay. In all cases, the IC_{50} values calculated using the MTT assay were within

10% of the values calculated by the crystal violet assay. We plated cells into 96-well plates and incubated them for 24 h under the conditions described above for standard cell culture maintenance. The cells were subsequently exposed to dasatinib at various concentrations for 72 h. Eight wells were treated at each concentration. After treatment with dasatinib, 25 μL of MTT was added to each well, and the wells were incubated for 3 h. The medium was then removed, and 100 μL of Me_2SO was added. The absorbance of individual wells was read at 490 nm.

Cell Cycle Analysis

Cells were plated in complete medium at 50% confluence the day before starting the experiment. Cells were synchronized by serum starvation for 24 h, followed by the restoration of complete medium for 12 h before the addition of 100 nmol/L dasatinib for 6 or 18 h (38). Cells were harvested, washed in PBS, fixed in 1% paraformaldehyde, rewashed in PBS, and resuspended in 70% ethanol at −20°C overnight. Cells were then washed twice with PBS and stained with 20 μg/mL propidium iodide. DNA content was analyzed on a cytofluorimeter by fluorescence-activated cell sorting analysis (FACScan; Becton Dickinson and Company) using ModFit software (Verity Software House).

Apoptosis Assay

Subconfluent cells were treated with 100 nmol/L dasatinib for 6 h. Cells were then harvested and stained with Annexin V and propidium iodide and analyzed on a cytofluorimeter by FACScan using ModFit software.

Migration Assay (Scratch Assay)

MPM cells were grown to confluence on tissue culture dishes, and a single scrape was made in the confluent monolayer using a sterile pipette tip. The monolayer was washed with PBS, and then complete medium containing 25 nmol/L (for MSTO-211H cells), 100 nmol/L (for other cell lines), or DMSO alone (vehicle control) was added. Lower dasatinib concentrations were used in the MSTO-211H cells to reduce cytotoxicity. Serial photographs of the same scraped section were taken every 6 h for 72 h (39). The number of cells that migrated over the margins of the wounds was counted after 6 h (40, 41). The time required for the scrape to close was also recorded.

Invasion Assay

The invasive capacity of mesothelioma cells was measured using a modified Boyden chamber (42). The chamber consisted of a porous filter (with pores 8 μm in diameter) that separated the chamber into two compartments. The top of the filter was coated with Matrigel. Cells to be assayed were placed in the upper compartment in complete medium, and serum-free medium was placed in the lower compartment; the cells were allowed to attach and spread for 16 h. Then, 25 nmol/L (MSTO-211H) or 100 nmol/L (other cell lines) dasatinib was added to the cells in the upper compartment, and 3T3 conditioned medium (as a chemoattractant) was placed in the bottom compartment. After 24 h of incubation under standard tissue culture conditions, cells on top of the filter (those that had not invaded through the filter) were scraped off and discarded. The remaining cells (i.e., those that had invaded through the Matrigel and the filter) were fixed, stained, and counted using light microscopy. In parallel experiments, cells from the same lines were treated identically in 24-well plates. These cells were harvested, stained with trypan blue, and counted. The number of cells that had invaded was normalized to analyze the effects on cell viability. Twenty random fields were chosen from each cell line and counted blindly. Experiments were done in duplicate.

Western Blot Analysis

Detached cells from each cell culture plate were collected by centrifugation, washed in PBS, and added to the cell lysate from their corresponding plates. Adherent cells were rinsed with ice-cold PBS and lysed in the cell culture plate for 20 min on ice in lysis buffer consisting of 50 mmol/L Trizma base (pH 8; Sigma Chemical Company), 1% Triton X-100, 150 mmol/L NaCl, 20 μg/mL leupeptin, 10 μg/mL aprotinin, 1 mmol/L phenylmethylsulfonyl fluoride, and 1 mmol/L sodium vanadate. Lysates were spun in a centrifuge at 14,000 rpm for 5 min, and the supernatant was collected. Equal protein aliquots were resolved by SDS-PAGE, transferred to nitrocellulose membranes, immunoblotted with primary antibody, and detected with horseradish peroxidase–conjugated secondary antibody (Bio-Rad Laboratories) and enzymatic chemiluminescence reagent (Amersham Biosciences).

DNA Extraction and c-Src Mutation Analysis

DNA was extracted from the cell lines using the DNeasy Tissue kit (Qiagen), and all PCR products were sequenced using Applied Biosystems PRISM dye terminator cycle-sequencing method (Perkin-Elmer Corp.). The entire exon 12 region of the *c-Src* gene was amplified by PCR using the following primers: sense (5′-ATGGTGAACCGCGAG-GTGCT) and antisense (5′-GATCCAAGCCGAGAAGCC-GGTCTG). For PCR amplification, 100 to 500 ng of genomic DNA was used; each amplification was done in a 40-μL volume containing 2.0 μL of DNA, 2.5 μL of each primer (20 pmol/L), 20 μL of HotStarTaq Master Mix (Qiagen), and 13 μL of DNase-free water. DNA was amplified for 35 cycles at 94°C for 30 s, 65°C for 30 s, and 72°C for 30 s, followed by 10-min extension at 72°C. All PCR products were directly sequenced using Applied Biosystems PRISM dye terminator cycle sequencing method (Perkin-Elmer Corp.).

Immunohistochemistry

For the immunohistochemical analyses, formalin-fixed paraffin-embedded mesothelioma cell pellets and 46 malignant mesothelioma tumors from the thoracic archival tissue bank at The University of Texas M.D. Anderson Cancer Center were evaluated. The tumor tissues were residual specimens from patients who underwent surgical resection (pleurectomy or extrapleural pneumonectomy) of their malignant mesothelioma at our institution. This project was approved by our institutional review board. The positive controls were non–small cell lung cancer cell lines and lung cancer tissues that overexpress c-Src and p-Src (43). Paraffin-embedded mesothelioma cell pellets and the MPM tumor blocks were cut into 4-μL sections

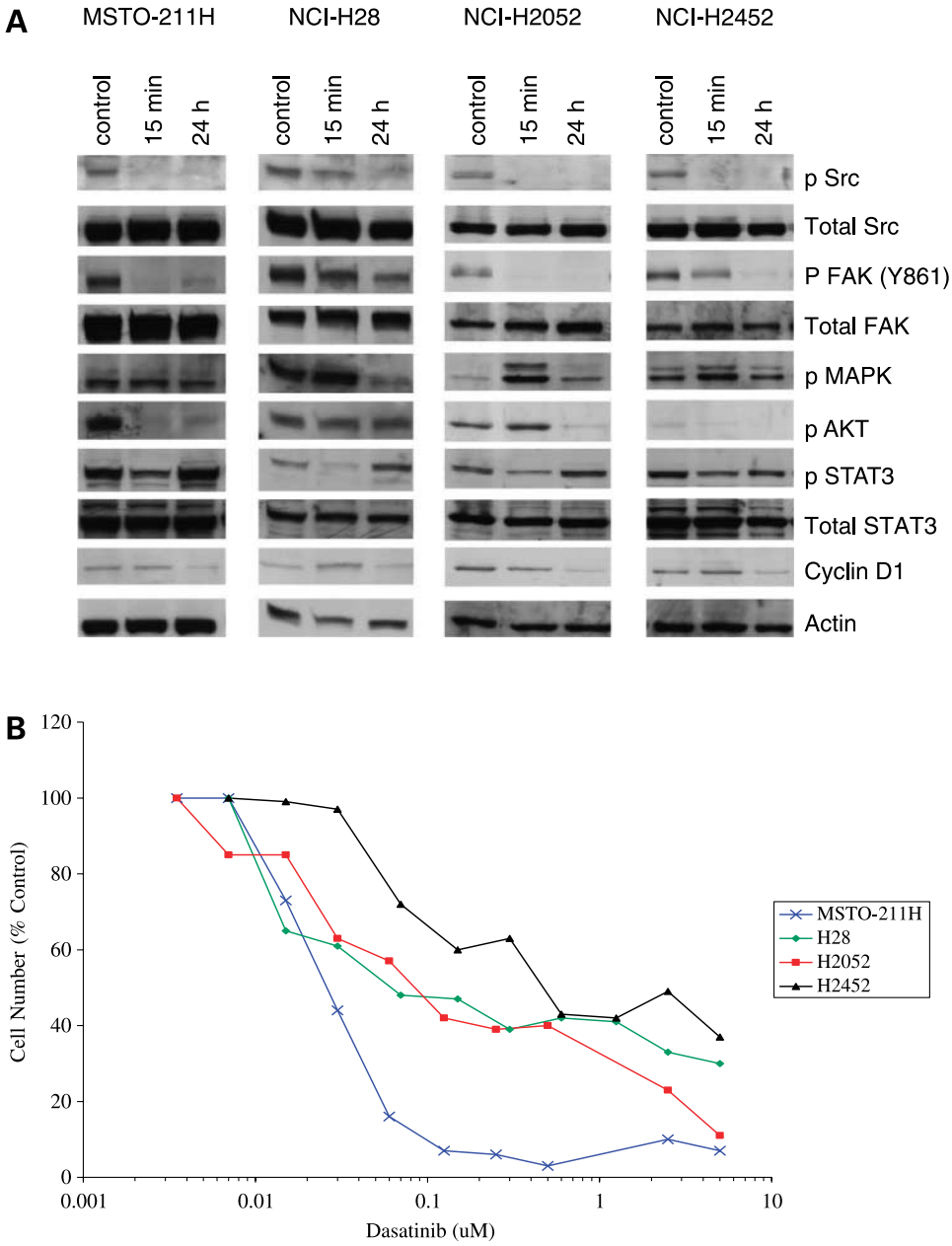

Figure 1. The effect of dasatinib on MPM cell downstream pathways and cytotoxicity. **A,** MPM cells were treated with 100 nmol/L dasatinib for the indicated times, lysed, and analyzed by Western blotting with the indicated antibodies. **B,** MPM cells were treated with dasatinib at the indicated concentrations for 72 h. Cell number was estimated using an MTT assay. Cells treated with vehicle alone were defined as 100%.

and then deparaffinized, rehydrated, and washed with TBS Tween 20. Antigens were retrieved with exposure to 1 mmol/L EDTA (pH 8.0; DakoCytomation) for 20 min in a steamer. Endogenous activity in samples was blocked by exposure to 3% hydrogen peroxide/PBS (Fisher Scientific, Fair Lawn, NJ) and Dako serum-free protein block (DakoCytomation). After this, samples were incubated with the primary antibodies (c-Src antibody, 1:100; p-Src

Table 1. Characteristics of four MPM cell lines and IC_{50} values to dasatinib therapy

Cell line	IC_{50} (nmol/L)	Histology	Patient characteristics
MSTO-211H	25	Biphasic	62-y-old male Caucasian
NCI-H28	60	Mesothelioma	48-y-old male Caucasian smoker
NCI-H2052	80	Mesothelioma	65-y-old male Caucasian smoker
NCI-H2452	980	Epithelioid	Male nonsmoker (age unknown)

family Y416 and Y527, 1:50) overnight at 4°C. Standard avidin/biotin immunoperoxidase methods with diaminobenzidines as the chromogen were used for detection (DakoCytomation). To analyze the specificity of the immunostaining results, we created negative controls by pretreating the samples with c-Src blocking peptide (Cell Signaling Technologies). c-Src and p-Src staining were quantified on the basis of the percentage of cells that stained in the cytoplasm and membrane. Both the extent and intensity of immunopositive staining were considered for both membrane and cytoplasmic immunostaining. The intensity of staining ranged from 0 to 3 and the extent from 0% to 100%. The final staining score (range 0–300) was obtained by multiplying the extent and intensity scores.

Statistical Analysis

A database containing clinical, demographic, and biomarker characteristics of the 46 patients with resected MPM from whom the tissue samples were obtained was analyzed to determine whether c-Src or p-Src (Y419 or Y530) on the cell membrane or in the cytoplasm is a prognostic factor for recurrence of disease or overall survival. This protocol was approved by the institutional review board at M. D. Anderson Cancer Center. The primary analysis was

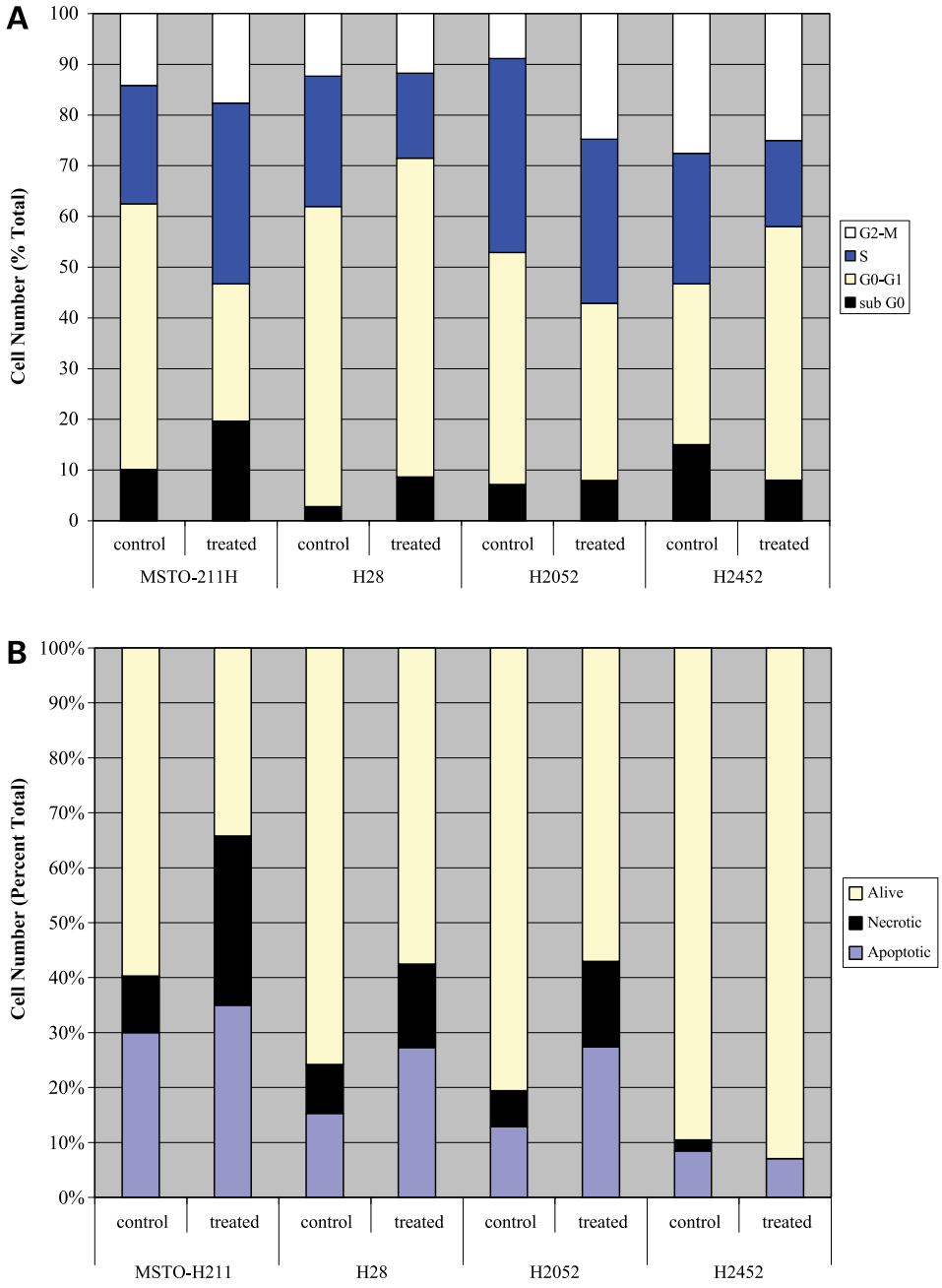

Figure 2. The effects of dasatinib on cell cycle and apoptosis. **A,** MPM cells (MSTO-211H, NCI-H28, NCI-H2052, NCI-H2452) were treated with 100 nmol/L dasatinib for 16 h before being stained with propidium iodide and analyzed with FACS to determine the proportion of cells in each phase of the cell cycle. **B,** MPM cells (MSTO-211H, NCI-H28, NCI-H2052, NCI-H2452) were treated with 100 nmol/L dasatinib for 6 h and stained with propidium iodide and Annexin V to estimate the number of necrotic cells (propidium iodide positive) and those that were undergoing early apoptosis (Annexin V positive). SFK inhibition in sensitive cell lines resulted in apoptosis and cell cycle arrest.

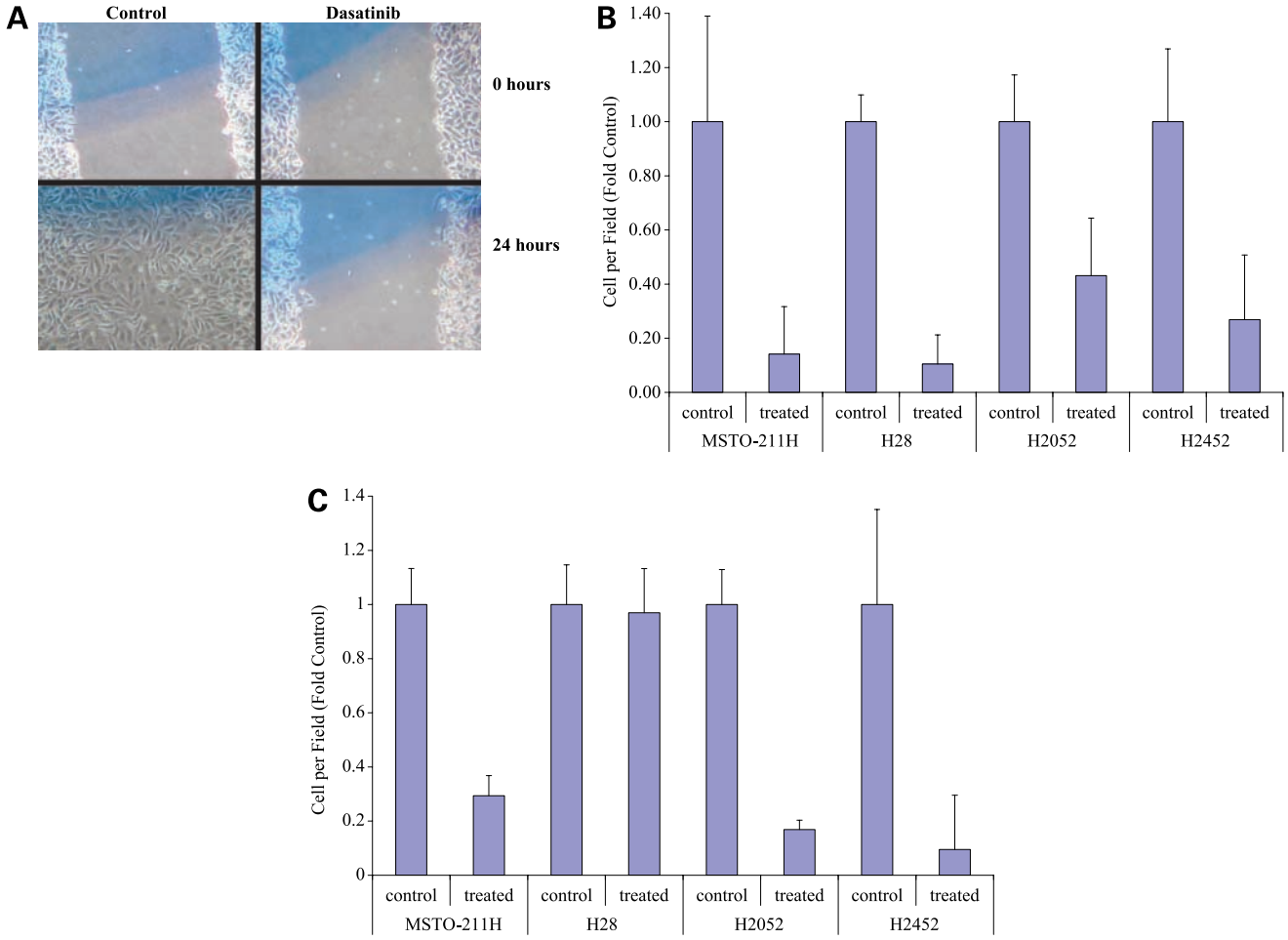

Figure 3. Effect of dasatinib on cell migration and invasion. **A,** MPM cells were plated to confluence on tissue culture plastic. A single scratch was made in the confluent monolayer. The scratch was monitored and photographed every 6 h for 24 h (representative data). **B,** cells that migrated into the scratch after 6 h were counted. The data represent two independent experiments. In each experiment, 20 fields were counted. *Bars,* SD. In all cases, when treated cells are compared with corresponding controls, $P < 0.05$. **C,** cells were plated onto Matrigel-coated filters in a modified Boyden chamber. Cells were allowed to attach and spread for 16 h before the addition of 25 nmol/L (MSTO-211H) or 100 nmol/L (all others) dasatinib to the upper chamber and conditioned medium to the lower chamber. After 24 h, cells still in the upper chamber were removed, and cells that had invaded through the Matrigel were stained and counted. In parallel, control cells treated identically were assessed for viability and cell number with trypan blue. The average number of cells per field is expressed as a percentage of the control after normalizing for cell number. In MSTO-211H, NCI-2052, and NCI-H2452 cells, dasatinib inhibited invasion compared with corresponding controls, $P < 0.05$.

conducted to determine if the intensity, extension, and total scores of c-Src or p-Src had any prognostic value. In addition to being treated as a continuous variable, the total score was dichotomized to be positive if greater than its median and negative if less than or equal to its median. Secondary analysis was conducted to determine the effects of all clinical variables (i.e., patient demographics, histology, pathology stage, location of recurrence, asbestos exposure, and smoking history) on recurrence and survival and to determine if the clinical variables were associated with the c-Src or p-Src (Y419 or Y530) immunohistochemical staining scores. The Kaplan-Meier method was used to estimate the survival function. The Cox model was used to determine the prognostic effects of biomarkers (c-Src and p-Src) and clinical variables. In addition, logistic regression, ANOVA between groups, and Spearman correlation were used to assess the association between biomarkers and other variables.

Results

c-Src Is Activated in MPM Cell Lines

We analyzed four MPM cell lines (MSTO-211H, NCI-H28, NCI-H2052, and NCI-H2452) for protein expression of total c-Src, p-Src Y530, and p-Src Y419 using immunohistochemical analysis of cell pellets. Total c-Src was highly expressed in all four cell lines. There was no phosphorylation of c-Src Y530 in any of the four cell lines and high p-Src Y419 expression in MSTO-211H and NCI-H2052, indicating c-Src activation (data not shown).

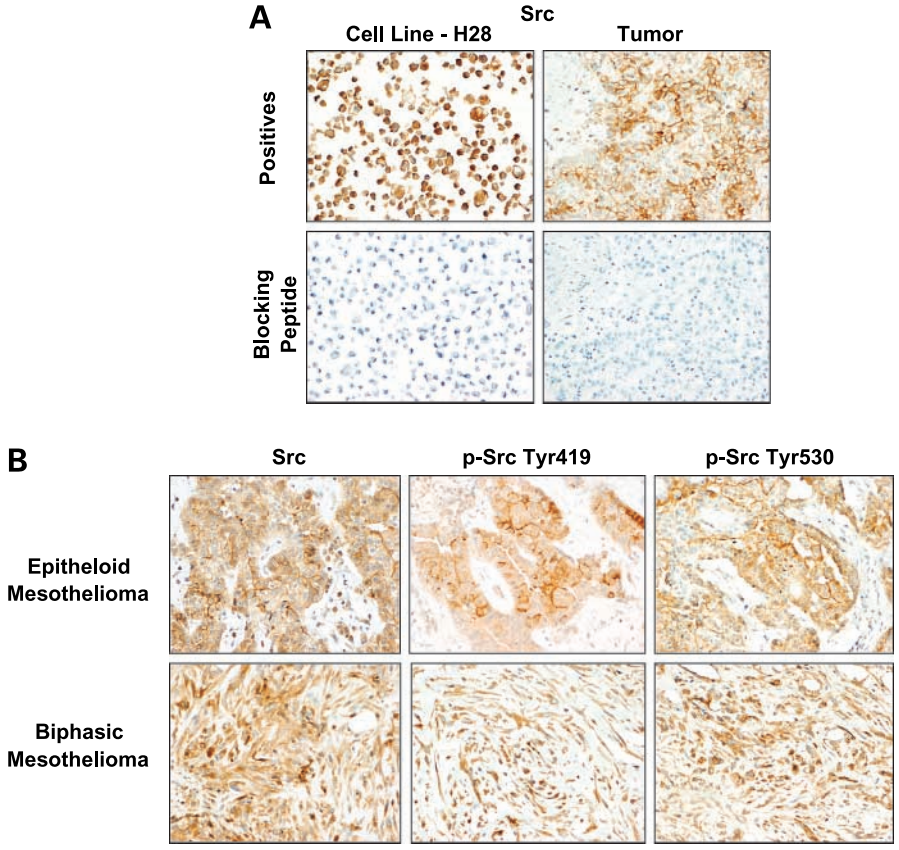

Figure 4. Representative examples of immunohistochemical analysis of MPM cell lines and tissue specimens. **A,** c-Src expression in MPM cell line H28 and one tumor specimen with positive membrane and cytoplasmic staining. As a control, blocking peptide shows the absence of immunostaining in both specimens. **B,** examples of immunostaining for the three antibodies used on MPM tissue specimens showing positive membrane and cytoplasmic staining in tumor cells.

Western blot analysis confirmed that total c-Src and activated c-Src (Y419) were expressed in all four cell lines (Fig. 1A).

Treatment with Dasatinib Induces Cell Cycle Arrest and Apoptosis in MPM Cell Lines

We treated the four MPM cell lines with dasatinib and used a crystal violet assay and an MTT assay to test for cytotoxicity (Fig. 1B). Three of the four cell lines had IC_{50} levels below 100 nmol/L, which suggests target specificity (Table 1); these levels are achieved in the serum of humans treated with dasatinib. Dasatinib (100 nmol/L) led to apoptosis and cell cycle arrest in the sensitive cell lines (Fig. 2). Consistent with the results of the cytotoxicity data, dasatinib had no effect on cell cycle or apoptosis in the insensitive cell line.

SFK Inhibition Causes Decreased Migration and Invasion

All four cell lines were treated with 25 to 100 nmol/L dasatinib, and cell migration was measured using the scratch assay described above (Fig. 3A). The number of cells that had migrated into the wound after 6 h was calculated and is shown in Fig. 3B. In all cell lines, dasatinib significantly inhibited cell migration. Cell number was not significantly affected after 6 h of treatment with 25 to 100 nmol/L dasatinib (data not shown). The kinetics of cell migration in the wound and the closure of the wound were also noted. There was complete wound closure within 24 to 36 h in all of the untreated cell lines but in none of the treated cell lines. Cell invasion, as measured using a modified Boyden chamber with a Matrigel-coated filter, was significantly inhibited by dasatinib in three of the four MPM cell lines (Fig. 3C).

Dasatinib Inhibits c-Src Activity and Downstream Signaling

The effects of dasatinib on cell signaling were evaluated in all four MPM cell lines with wide diversity in their antiproliferative or apoptotic sensitivity to dasatinib. The baseline levels of c-Src and activated c-Src (Y419) were measured by Western blotting (Fig. 1A). There was no consistent correlation between the expression or activation of c-Src at baseline and the biological effects of dasatinib in these cell lines. Dasatinib caused complete or near-complete and durable inhibition of c-Src activity in all cell lines, as measured by phosphorylation at Y419 in Western blotting. As expected, total c-Src levels were not affected. The effects of 100 nmol/L dasatinib on known downstream targets of c-Src were examined by Western blotting in cells treated for 15 min and 24 h (Fig. 1A). In all cell lines, FAK phosphorylation was decreased at an Src-dependent site (Y861) and cyclin D1 expression was decreased. Mitogen-activated protein kinase activity was transiently increased in most MPM cell lines; STAT3 activation was transiently reduced and returned to baseline levels within 24 h; and inhibition of AKT phosphorylation was variable, which is

consistent with the effects of dasatinib in head and neck squamous cell carcinoma and non–small cell lung cancer cell lines (44).

Activated c-Src Correlates with Higher Pathologic Stage and Presence of Metastasis in Human MPM Tissue

We conducted immunohistochemical analyses (total c-Src, p-Src Y419, p-Src Y530) of 46 human MPM samples obtained during surgical resection and archived in our tissue bank (Fig. 4). Twenty-six patients had epithelioid histology, 14 had biphasic tumors, and 6 had sarcomatoid tumors. In this cohort of patients (Table 2), the mean and median patient age was 60 years (range, 37–78 years). Eighty-three percent of these patients had no prior therapy before surgery, and only eight (17%) patients received neoadjuvant chemotherapy (one of these patients had a partial response). Nine percent of patients had residual disease at the time of surgery, and 57% of patients developed recurrent disease after curative intent surgery. At a median follow-up of 37.3 months, 41 patients had died: 68% from recurrent or progressive MPM, 25% from treatment-related causes, and 7% from unknown causes. Consistent with the literature, higher nodal status and nonepithelial histology were independent adverse prognostic factors. The hazard ratio for cancer relapse increased with N stage; the hazard ratio was 1.67 ($P = 0.05$) for each one-stage increase in N stage. The death hazard ratio in patients with epithelial histology versus patients with biphasic tumors was 0.63 ($P = 0.04$; i.e., patients with epithelial histology have a risk of death that is 63% that of the risk of death in patients with biphasic tumors).

The c-Src protein was expressed in the membrane in 39 of the 46 MPM tumor specimens and in the cytoplasm of all tumor specimens. There was positive p-Src Y419 expression on the membrane in 43% (20 of 46) and in the cytoplasm in 67% (31 of 46) of the MPM tumors. When the total scores were evaluated as a continuous variable, there was a statistically significant association between greater p-Src Y419 membrane staining and a more advanced pathologic stage ($P = 0.05$; Table 3). The p-Src Y419 staining score for the membrane was highest in patients with stage IV disease. In addition, the presence of metastasis (M stage) was associated with higher membrane scores of p-Src Y419 ($P = 0.03$) and higher cytoplasmic expression of p-Src Y419 ($P = 0.04$).

There were nine tumors that expressed p-Src Y530 on the membrane, and 13 tumors (the nine included) that expressed p-Src Y530 in the cytoplasm. Loss of phosphorylation at p-Src Y530 on the membrane was associated with higher nodal status. Specimens with N_1 nodal disease had the highest level of expression of membrane p-Src Y530, and specimens with N_2 nodal disease had the lowest expression ($P = 0.02$). In 11 of the tumors with p-Src Y530 expression, concurrent activation with p-Src Y419 was seen.

There was no other statistically significant association between the phosphorylation status of c-Src and patient demographics. There was, however, a trend toward a decrease in the expression of p-Src Y419 in the cytoplasm in patients exposed to asbestos and in those with greater smoking pack-years (correlation coefficient = −0.28; $P = 0.06$).

Forty-two of the 46 patients were disease-free after surgery. Of the 42 patients, 26 (62%) developed disease recurrence by the time of this study, with a median time to recurrence of 7.82 months. Eighty-nine percent (41 of 46) of the patients died, for a median overall survival duration of 7.52 months after surgery. There was no association between the level of c-Src activation and increased risk of disease relapse, site of relapse (local, regional, distant), or overall survival.

Table 2. Clinical and demographic patient data

Characteristic	*n* Patients	Percent of total (%)
Sex		
Female	8	17
Male	38	83
Ethnicity		
African-American	1	2
Hispanic	1	2
Caucasian	44	96
Prior cancer		
None	39	85
Aerodigestive tract	0	0
Other (i.e., skin)	7	15
Family history of MPM		
No	44	96
Yes	2	4
Asbestos exposure		
No	14	31
Yes	31	67
Unknown	1	2
Smoking status		
Current	6	13
Former	24	52
Never	16	35
Surgery		
Extrapleural pneumonectomy	42	91
Pleurectomy	4	9
Side of resected tumor		
Right	26	57
Left	20	43
Pathologic stage		
II	1	2
III	29	63
IV	16	35
Pathologic T stage		
T_2	10	22
T_3	25	54
T_4	11	24
Pathologic N stage		
N_0	20	43
N_1	6	13
N_2	20	43
Pathologic M stage		
M_0	39	85
M_1	7	15

Table 3. ***P*** **values for the associations between Src expression/activation and disease stage**

Stage	Src membrane	Src cytoplasm	Src Y 419 membrane	Src Y 419 cytoplasm	Src Y 530 membrane	Src Y 530 cytoplasm
Pathologic stage	0.93	0.22	0.05	0.19	0.36	0.18
T stage	0.6	0.23	0.57	0.09	0.59	0.43
N stage	0.45	0.96	0.74	0.09	0.02	0.07
M stage	0.62	0.99	0.03	0.04	0.79	0.28

MPM Tissues and Cell Lines Do Not Harbor c-Src Mutations in Exon 12

No gene mutations in *c-Src* exon 12 were found in any of the four cell lines. *c-Src* gene was sequenced in all 46 human tumor specimens (data not shown); there were no mutations found in *c-Src* exon 12.

Discussion

Our findings show that c-Src is commonly expressed and activated in MPM cell lines and tissue samples by dephosphorylation of the regulatory Y530 site and phosphorylation at the Tyr^{419} site. Activation of c-Src correlated with distant (p-Src 419) and nodal (loss of p-Src 530) metastases. This is consistent with the known role of c-Src in cancer cell invasion and metastasis.

Treatment of the MPM cell lines with the SFK inhibitor dasatinib showed promising cytotoxic effects, with IC_{50} values below achievable serum levels and abrogation of c-Src downstream signaling. In sensitive cell lines, dasatinib led to significant apoptosis and cell cycle arrest. Our *in vitro* work suggests that this agent should be evaluated further in animal studies and clinical trials.

STAT3 inhibition did not follow the durable inhibition of c-Src after incubation with dasatinib. This reactivation of STAT3 may be a compensatory response to suppress the proapoptotic or antiproliferative effects of dasatinib. Although unexpected in this study, the lack of long-term STAT3 inhibition has been observed in multiple tumor types (44, 45).[5] Combining STAT3 inhibitors with dasatinib may lead to synergistic antitumor effects in MPM, and this strategy is currently being examined. Thus, our findings provide evidence that targeting multiple pathways in solid tumors may be the most effective therapeutic strategy.

Src expression and inhibition did not predict changes in cell cycle arrest, apoptosis, or growth inhibition in response to dasatinib in these cell lines. The diversity of biological and molecular responses to dasatinib was not unexpected and has been seen in other tumor types (44, 45) and with other kinase inhibitors. For example, EGFR inhibitors also show diverse biological and molecular effects in patient tumors and cell lines that are independent of the degree of EGFR expression (46, 47). Although some of this may be due to EGFR mutation, an uncoupling of EGFR inhibition from downstream biological effects is also seen in many cell lines (2, 44, 47–49).

In this study, there was no association between the activation of c-Src and clinical outcomes in patients from whom the tumor specimens were obtained. This may be because we had a small, homogeneous sample, with two thirds of the patients' tumors being activated at Y419. Our tissue specimens are one limitation of this retrospective study. Although the archival tissues were chosen at random from our tissue bank, our patient demographics favor Caucasian men, and there was a higher ratio of biphasic and sarcomatoid tumors in our study than in the general population; biphasic and sarcomatoid tumors are associated with a worse prognosis than are epithelial tumors. Also, evaluating phosphorylated antibodies in archived paraffin tumors is problematic, as it has been discovered that the length of time between when a tumor is removed from the body and when it is evaluated can affect the phosphorylation status of the receptor (50). Our archival tissues were collected over several years, before this was known, and the time between removal from the body and tissue fixation is unknown. Therefore, we must cautiously interpret the prognostic value of the phosphorylated molecule, and prospective trials with controlled conditions are needed to validate the results of this study.

Despite the limitations of our study, our findings are compelling. First, we found that c-Src is a potential therapeutic target in MPM, and targeting c-Src in the induction or adjuvant setting to prevent metastasis or even stabilize disease by preventing local cell invasion would be reasonable. Multimodality therapy that includes systemic treatment is clearly necessary to control this disease. This has been evidenced by the results of clinical trials of curative intent surgery plus adjuvant radiotherapy in which the rate of recurrent MPM in a distant site has been as high as 50% (51, 52). To further assess the therapeutic effects of SFK inhibition, we plan to conduct a clinical trial at our institution using induction of the single-agent dasatinib in patients with resectable MPM.

Second, our data suggest that the combination of SFK inhibitors with other agents, such as STAT3 inhibitors (44, 45), may lead to enhanced cytotoxic effects. There is a growing body of evidence suggesting that c-Src inhibition has greater potential for preventing tumor metastasis rather than directly affecting the growth of the primary tumor (53). Therefore, targeting c-Src in combination with inhibition of other carcinogenic regulatory pathways may be the most advantageous therapeutic strategy.

[5] Johnson FM, Saigal B, Tran HT, Donato NJ. Abrogation of STAT3 reactivation after Src kinase inhibition results in synergistic antitumor effects. Clin Cancer Res. In press, 2007.

Dasatinib may also affect MPM cells and tumors through other kinases. MPM expresses platelet-derived growth factor and its receptor (22–31). Platelet-derived growth factor is a mitogen for MPM cells, and some studies suggest that it is an autocrine loop pathway for tumor cell proliferation and angiogenesis (24–26, 44, 54–59). Ephrin kinases (EPHA, EPHB) are thought to promote angiogenesis and enhance tumor cell motility, invasion, and metastasis (60–63). EPHB4, a receptor tyrosine kinase, is associated with vascular remodeling (64) and has recently been shown to be highly expressed in mesothelioma cell lines and primary tumor tissues (65). The c-Kit tyrosine kinase receptor and its downstream mediator Slug, a zinc finger transcription factor, are involved in cell survival, proliferation, adhesion, and differentiation (66). Recent studies have suggested that Slug is an important regulator of epithelial-mesenchymal transitions in tumor progression (6), and *in vitro* data suggest that this pathway plays a role in multidrug resistance in mesothelioma cells.

In conclusion, we found that SFK inhibition with dasatinib led to cell cycle arrest, apoptosis, and inhibition of migration and invasion in MPM cell lines. The expression of c-Src was common in MPM tissues, and activation correlated with advanced pathologic stage. This shows that c-Src is a potential therapeutic target in MPM. This is the first published study to comprehensively evaluate c-Src expression and activation in MPM and investigate the therapeutic role of c-Src inhibition in MPM.

References

1. Herndon JE, Green MR, Chahinian AP, Corson JM, Suzuki Y, Vogelzang NJ. Factors predictive of survival among 337 patients with mesothelioma treated between 1984 and 1994 by the Cancer and Leukemia Group B. Chest 1998;113:723–31.

2. Rusch VW, Rosenzweig K, Venkatraman E, et al. A phase II trial of surgical resection and adjuvant high-dose hemithoracic radiation for malignant pleural mesothelioma. J Thorac Cardiovasc Surg 2001;122:788–95.

3. Vogelzang NJ, Rusthoven JJ, Symanowski J, et al. Phase III study of pemetrexed in combination with cisplatin versus cisplatin alone in patients with malignant pleural mesothelioma. J Clin Oncol 2003;21:2636–44.

4. Irby RB, Yeatman TJ. Role of Src expression and activation in human cancer. Oncogene 2000;19:5636–42.

5. Levin VA. Basis and importance of Src as a target in cancer. Cancer Treat Res 2004;119:89–119.

6. Thiery JP. Epithelial-mesenchymal transitions in tumour progression. Nat Rev Cancer 2002;2:442–54.

7. Thompson EW, Newgreen DF, Tarin D. Carcinoma invasion and metastasis: a role for epithelial-mesenchymal transition? Cancer Res 2005;65:5991–5; discussion 5995.

8. Eliceiri BP, Paul R, Schwartzberg PL, Hood JD, Leng J, Cheresh DA. Selective requirement for Src kinases during VEGF-induced angiogenesis and vascular permeability. Mol Cell 1999;4:915–24.

9. Yezhelyev MV, Koehl G, Guba M, et al. Inhibition of SRC tyrosine kinase as treatment for human pancreatic cancer growing orthotopically in nude mice. Clin Cancer Res 2004;10:8028–36.

10. Summy JM, Trevino JG, Lesslie DP, et al. AP23846, a novel and highly potent Src family kinase inhibitor, reduces vascular endothelial growth factor and interleukin-8 expression in human solid tumor cell lines and abrogates downstream angiogenic processes. Mol Cancer Ther 2005;4:1900–11.

11. Trevino JG, Summy JM, Gray MJ, et al. Expression and activity of SRC regulate interleukin-8 expression in pancreatic adenocarcinoma cells: implications for angiogenesis. Cancer Res 2005;65:7214–22.

12. Gray MJ, Zhang J, Ellis LM, et al. HIF-1α, STAT3, CBP/p300 and Ref-1/APE are components of a transcriptional complex that regulates Src-dependent hypoxia-induced expression of VEGF in pancreatic and prostate carcinomas. Oncogene 2005;24:3110–20.

13. Summy JM, Trevino JG, Baker CH, Gallick GE. c-Src regulates constitutive and EGF-mediated VEGF expression in pancreatic tumor cells through activation of phosphatidyl inositol-3 kinase and p38 MAPK. Pancreas 2005;31:263–74.

14. Trevino JG, Summy JM, Lesslie DP, et al. Inhibition of SRC expression and activity inhibits tumor progression and metastasis of human pancreatic adenocarcinoma cells in an orthotopic nude mouse model. Am J Pathol 2006;168:962–72.

15. Johnson FM, Gallick GE. Src Family Nonreceptor Tyrosine Kinases as Molecular Targets for Cancer Therapy. Curr Med Chem. In press 2007.

16. Turkson J, Bowman T, Garcia R, Caldenhoven E, De Groot RP, Jove R. Stat3 activation by Src induces specific gene regulation and is required for cell transformation. Mol Cell Biol 1998;18:2545–52.

17. Karni R, Jove R, Levitzki A. Inhibition of pp60c-Src reduces Bcl-XL expression and reverses the transformed phenotype of cells overexpressing EGF and HER-2 receptors. Oncogene 1999;18:4654–62.

18. Yeatman TJ. A renaissance for SRC. Nat Rev Cancer 2004;4:470–80.

19. Tan YX, Wang HT, Zhang P, et al. c-Src activating mutation analysis in Chinese patients with colorectal cancer. World J Gastroenterol 2005;11:2351–3.

20. Irby RB, Mao W, Coppola D, et al. Activating SRC mutation in a subset of advanced human colon cancers. Nat Genet 1999;21:187–90.

21. Laghi L, Bianchi P, Orbetegli O, Gennari L, Roncalli M, Malesci A. Lack of mutation at codon 531 of SRC in advanced colorectal cancers from Italian patients. Br J Cancer 2001;84:196–8.

22. Ohta Y, Shridhar V, Bright RK, et al. VEGF and VEGF type C play an important role in angiogenesis and lymphangiogenesis in human malignant mesothelioma tumours. Br J Cancer 1999;81:54–61.

23. Kumar-Singh S, Vermeulen PB, Weyler J, et al. Evaluation of tumour angiogenesis as a prognostic marker in malignant mesothelioma. J Pathol 1997;182:211–6.

24. Langerak AW, De Laat PA, Van Der Linden-Van Beurden CA, et al. Expression of platelet-derived growth factor (PDGF) and PDGF receptors in human malignant mesothelioma *in vitro* and *in vivo*. J Pathol 1996;178:151–60.

25. Konig JE, Tolnay E, Wiethege T, Muller KM. Expression of vascular endothelial growth factor in diffuse malignant pleural mesothelioma. Virchows Arch 1999;435:8–12.

26. Strizzi L, Catalano A, Vianale G, et al. Vascular endothelial growth factor is an autocrine growth factor in human malignant mesothelioma. J Pathol 2001;193:468–75.

27. Kumar-Singh S, Weyler J, Martin MJ, Vermeulen PB, Van Marck E. Angiogenic cytokines in mesothelioma: a study of VEGF, FGF-1 and -2, and TGF β expression. J Pathol 1999;189:72–8.

28. Zebrowski BK, Yano S, Liu W, et al. Vascular endothelial growth factor levels and induction of permeability in malignant pleural effusions. Clin Cancer Res 1999;5:3364–8.

29. Senger DR, Galli SJ, Dvorak AM, Perruzzi CA, Harvey VS, Dvorak HF. Tumor cells secrete a vascular permeability factor that promotes accumulation of ascites fluid. Science 1983;219:983–5.

30. Ferrara N, Gerber HP, LeCouter J. The biology of VEGF and its receptors. Nat Med 2003;9:669–76.

31. Kindler HL. Moving beyond chemotherapy: novel cytostatic agents for malignant mesothelioma. Lung Cancer 2004;45 Suppl 1:S125–7.

32. England JM, Panella MJ, Ewert DL, Halpern MS. Induction of a diffuse mesothelioma in chickens by intraperitoneal inoculation of v-src DNA. Virology 1991;182:423–9.

33. Miura Y, Nishimura Y, Katsuyama H, et al. Involvement of IL-10 and Bcl-2 in resistance against an asbestos-induced apoptosis of T cells. Apoptosis 2006;11:1825–35.

34. Poulikakos PI, Xiao GH, Gallagher R, Jablonski S, Jhanwar SC, Testa JR. Re-expression of the tumor suppressor NF2/merlin inhibits invasiveness in mesothelioma cells and negatively regulates FAK. Oncogene 2006;25:5960–8.

35. Lombardo LJ, Lee FY, Chen P, et al. Discovery of N-(2-chloro-6-methyl-phenyl)-2-(6-(4-(2-hydroxyethyl)- piperazin-1-yl)-2-methylpyrimidin-4-ylamino)thiazole-5-carboxamide (BMS-354825), a dual Src/Abl

kinase inhibitor with potent antitumor activity in preclinical assays. J Med Chem 2004;47:6658 – 61.

36. Talpaz M, Shah NP, Kantarjian H, et al. Dasatinib in imatinib-resistant Philadelphia chromosome-positive leukemias. N Engl J Med 2006;354: 2531 – 41.

37. Mujoo K, Maneval DC, Anderson SC, Gutterman JU. Adenoviral-mediated p53 tumor suppressor gene therapy of human ovarian carcinoma. Oncogene 1996;12:1617 – 23.

38. Campisi J, Morreo G, Pardee AB. Kinetics of G_1 transit following brief starvation for serum factors. Exp Cell Res 1984;152:459 – 62.

39. Kong-Beltran M, Stamos J, Wickramasinghe D. The Sema domain of Met is necessary for receptor dimerization and activation. Cancer Cell 2004;6:75 – 84.

40. Michieli P, Mazzone M, Basilico C, et al. Targeting the tumor and its microenvironment by a dual-function decoy Met receptor. Cancer Cell 2004;6:61 – 73.

41. Beaudry P, Force J, Naumov GN, et al. Differential effects of vascular endothelial growth factor receptor-2 inhibitor ZD6474 on circulating endothelial progenitors and mature circulating endothelial cells: implications for use as a surrogate marker of antiangiogenic activity. Clin Cancer Res 2005;11:3514 – 22.

42. Albini A, Iwamoto Y, Kleinman HK, et al. A rapid *in vitro* assay for quantitating the invasive potential of tumor cells. Cancer Res 1987;47: 3239 – 45.

43. Zhang J, Kalyankrishna S, Wislex M, et al. Src-family kinases are activated in non-small cell lung cancer and promote the survival of epidermal growth factor receptor-dependent cell lines. Am J Pathol 2007; 170:1 – 11.

44. Johnson FM, Saigal B, Talpaz M, Donato NJ. Dasatinib (BMS-354825) tyrosine kinase inhibitor suppresses invasion and induces cell cycle arrest and apoptosis of head and neck squamous cell carcinoma and non-small cell lung cancer cells. Clin Cancer Res 2005;11:6924 – 32.

45. Nam S, Kim D, Cheng JQ, et al. Action of the Src family kinase inhibitor, dasatinib (BMS-354825), on human prostate cancer cells. Cancer Res 2005;65:9185 – 9.

46. Wakeling AE, Guy SP, Woodburn JR, et al. ZD1839 (Iressa): an orally active inhibitor of epidermal growth factor signaling with potential for cancer therapy. Cancer Res 2002;62:5749 – 54.

47. Janmaat ML, Kruyt FA, Rodriguez JA, Giaccone G. Response to epidermal growth factor receptor inhibitors in non-small cell lung cancer cells: limited antiproliferative effects and absence of apoptosis associated with persistent activity of extracellular signal-regulated kinase or Akt kinase pathways. Clin Cancer Res 2003;9:2316 – 26.

48. Le Chevalier T, Lynch T. Adjuvant treatment of lung cancer: current status and potential applications of new regimens. Lung Cancer 2004;46 Suppl 2:S33 – 9.

49. Paez JG, Janne PA, Lee JC, et al. EGFR mutations in lung cancer: correlation with clinical response to gefitinib therapy. Science 2004;304: 1497 – 500.

50. Massarelli E, Onn A, Herbst R, et al. The time of tissue processing for human surgical specimens influences the level of epidermal growth factor receptor phosphorylation [Abstract 430]. In: Proceedings of the American Association of Cancer Research; 2005.

51. Stevens C, Rice D, Forster K, et al. Extrapleural pneumonectomy followed by IMRT: results of a phase I/II study [abstract 7178]. In: Proceedings of the American Society of Clinical Oncology; 2005.

52. Allen A, Den R, Wong J, et al. The influence of radiotherapy technique and dose on the patterns of failure for mesothelioma patients following extrapleural pneumonectomy [abstract #7094]. ASCO Annual Meeting Proceedings. J Clin Oncol 2006;24:7094.

53. Criscuoli ML, Nguyen M, Eliceiri BP. Tumor metastasis but not tumor growth is dependent on Src-mediated vascular permeability. Blood 2005; 105:1508 – 14.

54. Masood R, Kundra A, Zhu S, et al. Malignant mesothelioma growth inhibition by agents that target the VEGF and VEGF-C autocrine loops. Int J Cancer 2003;104:603 – 10.

55. Roberts F, Harper CM, Downie I, Burnett RA. Immunohistochemical analysis still has a limited role in the diagnosis of malignant mesothelioma. A study of thirteen antibodies. Am J Clin Pathol 2001;116: 253 – 62.

56. Nowak AK, Lake RA, Kindler HL, Robinson BW. New approaches for mesothelioma: biologics, vaccines, gene therapy, and other novel agents. Semin Oncol 2002;29:82 – 96.

57. Gerwin BI, Lechner JF, Reddel RR, et al. Comparison of production of transforming growth factor-β and platelet-derived growth factor by normal human mesothelial cells and mesothelioma cell lines. Cancer Res 1987;47: 6180 – 4.

58. Dorai T, Kobayashi H, Holland JF, Ohnuma T. Modulation of platelet-derived growth factor-β mRNA expression and cell growth in a human mesothelioma cell line by a hammerhead ribozyme. Mol Pharmacol 1994; 46:437 – 44.

59. Mutsaers SE, McAnulty RJ, Laurent GJ, Versnel MA, Whitaker D, Papadimitriou JM. Cytokine regulation of mesothelial cell proliferation *in vitro* and *in vivo*. Eur J Cell Biol 1997;72:24 – 9.

60. Dodelet VC, Pasquale EB. Eph receptors and ephrin ligands: embryogenesis to tumorigenesis. Oncogene 2000;19:5614 – 9.

61. Pandey A, Shao H, Marks RM, Polverini PJ, Dixit VM. Role of B61, the ligand for the Eck receptor tyrosine kinase, in TNF-α-induced angiogenesis. Science 1995;268:567 – 9.

62. Miao H, Burnett E, Kinch M, Simon E, Wang B. Activation of EphA2 kinase suppresses integrin function and causes focal-adhesion-kinase dephosphorylation. Nat Cell Biol 2000;2:62 – 9.

63. Andres AC, Reid HH, Zurcher G, Blaschke RJ, Albrecht D, Ziemiecki A. Expression of two novel eph-related receptor protein tyrosine kinases in mammary gland development and carcinogenesis. Oncogene 1994;9: 1461 – 7.

64. Gerety SS, Wang HU, Chen ZF, Anderson DJ. Symmetrical mutant phenotypes of the receptor EphB4 and its specific transmembrane ligand ephrin-B2 in cardiovascular development. Mol Cell 1999;4:403 – 14.

65. Xia G, Kumar SR, Masood R, et al. Up-regulation of EphB4 in mesothelioma and its biological significance. Clin Cancer Res 2005;11: 4305 – 15.

66. Catalano A, Rodilossi S, Rippo MR, Caprari P, Procopio A. Induction of stem cell factor/c-Kit/slug signal transduction in multi-drug-resistant malignant mesothelioma cells. J Biol Chem 2004;279: 46706 – 14.